International Conference on Mathematics, Computational Methods & Reactor Physics (M&C 2009)
Saratoga Springs, New York, May 3-7, 2009, on CD-ROM, American Nuclear Society, LaGrange Park, IL (2009)

A SIMPLIFIED 2D HTTR BENCHMARK PROBLEM

Zhan Zhang, Farzad Rahnema*, Justin M. Pounders, Dingkang Zhang
Nuclear and Radiological Engineering and Medical Physics Programs,
George W. Woodruff School
Georgia Institute of Technology, Atlanta, Georgia, 30332
Farzad@gatech.edu

Abderrafi Ougouag
Idaho National Laboratory
2525 North Freemont Avenue, Idaho Falls, IDAHO 83401
Abderrafi.Ougouag@inl.gov

ABSTRACT

To access the accuracy of diffusion or transport methods for reactor calculations, it is desirable to create heterogeneous benchmark problems that are typical of relevant whole core configurations. In this paper we have created a numerical benchmark problem in 2D configuration typical of a high temperature gas cooled prismatic core. This problem was derived from the HTTR start-up experiment. For code-to-code verification, complex details of geometry and material specification of the physical experiments are not necessary. To this end, the benchmark problem presented here is derived by simplifications that remove the unnecessary details while retaining the heterogeneity and major physics properties from the neutronics viewpoint. Also included here is a six-group material (macroscopic) cross section library for the benchmark problem. This library was generated using the lattice depletion code HELIOS. Using this library, benchmark quality Monte Carlo solutions are provided for three different configurations (all-rods-in, partially-controlled and all-rods-out). The reference solutions include the core eigenvalue, block (assembly) averaged fuel pin fission density distributions, and absorption rate in absorbers (burnable poison and control rods).

Key Words: VHTR, HTTR, heterogeneous benchmark, hexagonal geometry

1. INTRODUCTION

The development of new-generation reactors requires advanced methods with higher accuracy than traditional diffusion methods. To verify these new methods, it is desirable to create some new heterogeneous benchmark problems that exhibit features of these new reactor designs, an example of which is the Very High Temperature Reactor (VHTR). Many are working on extending existing diffusion methods or developing new transport methods for neutronics analysis of these reactors with higher accuracy on more complicated calculations. To test the accuracy of these modern methods, we have created a new heterogeneous benchmark problem that is typical of a high temperature reactor in hexagonal geometry.

* Corresponding author

The starting point for our benchmark problem was the experimental High Temperature Engineering Test Reactor (HTTR [1]), which was built by JAERI in the late 1990's. The HTTR is a high-temperature gas-cooled prismatic reactor and thus shares many of the same design features as the VHTR. In the HTTR, helium gas works as the coolant, and graphite blocks serve as the moderator, reflector and structure material. The fuel pins consist of fuel compacts, which are composed of coated UO_2 fuel particles and graphite matrix. Burnable poison (BP) rods are composed of boron carbide and carbon. Control rods (CR) consist of B_4C and carbon inside of an Alloy 800H sleeve.

Many calculations and simulations were conducted before and after the start-up experiments of HTTR to assist both in the design of these experiments and the validation of the numerical calculations. Many benchmarks describing the HTTR facility with varying levels of complexity were developed by international groups in Japan, France, Germany, Netherlands, Russia, USA, and other countries [2-4]. These benchmarks are true-to-design problems in that their goal was to explicitly model the HTTR with a high level of reactor specific detail.

For the purpose of new fundamental methods development, however, the high level of HTTR-specific details that exists in the current benchmark problems is unnecessary. The goal of new methods development is to create methodologies that are applicable to a general physical regime and not necessarily to a specific realization of a reactor. It is beneficial, therefore, for a generic benchmark problem to capture the fundamental physics of a reactor, while eliminating design-specific details that do not contribute to the fundamental physics and may, in fact, prove to be needlessly cumbersome at early stages of development. With this goal in mind, we have developed a 2D simplified HTTR benchmark that retains significant features (from a neutronics point of view) such as high heterogeneity, strong absorption regions and hexagonal geometry.

2. BENCHMARK PROBLEM DISCRIPTION

2.1. Simplification Methods

The following simplifications were made to the original HTTR start-up benchmark [1] to arrive at the simplified 2D HTTR benchmark.

1) Compositions and impurities of graphite were simplified to two typical values, instead of the ten as-built values that are very close to each other. Graphite in fuel blocks is chosen as typical value of low-impurity graphite, and its composition is used for all graphite blocks except the permanent reflector blocks, which have higher impurity.
2) Some geometric details were neglected, including gaps between blocks, plugs in fuel holes, dowels in BP holes, handling holes in blocks, neutron shielding pins in the bottom, and a few other minor geometric details. These particular design features have few physical effects on the active core, but highly aggravate the complexity of the benchmark.
3) The fuel blocks were made symmetric by averaging the burnable poison concentrations over all three BP cells. The number of control rod holes per control rod block was also reduced from three to one. This block symmetrization results in 60-degree rotational symmetry for the core.

4) The double heterogeneity effect was neglected for the sake of simplicity: coated fuel particles and the graphite matrix were homogenized into a mixed fuel material.
5) Material compositions were homogenized axially so that the original 3D benchmark is reduced to 2D. As a result, the number of different fuel block enrichments was reduced from twelve to four, and the number of BP was reduced from two to one.
6) The radial shape of the full core model was chosen to be hexagonal rather than the 12-edge polygonal shape of the original design. This simplification makes it is easier for most diffusion and transport codes to model the geometry and the external boundary condition.

2.2. Detailed Geometry Specification

The present benchmark problem is a whole-core heterogeneous 2D configuration in hexagonal geometry as shown in Fig. 1 (a). The reactor core is modeled as a regular hexagon with a flat-to-flat distance of 436.4768 cm and is completely filled by a hexagonal lattice of fuel, control and reflector blocks. These hexagonal blocks are all of uniform size with a flat-to-flat distance of 36 cm, except at the periphery in which case there are half blocks along the core edges and 1/3 blocks at the corners.

The block lattice configuration is shown in Fig. 1(b). Regions 1 through 4 in this figure are fuel blocks of increasing enrichment. Regions 5 and 6 are filled or empty control rod blocks depending on the core configuration. Regions 7 and 8 are replaceable and permanent reflector blocks, respectively. Vacuum boundary conditions are prescribed on the external boundaries of the core.

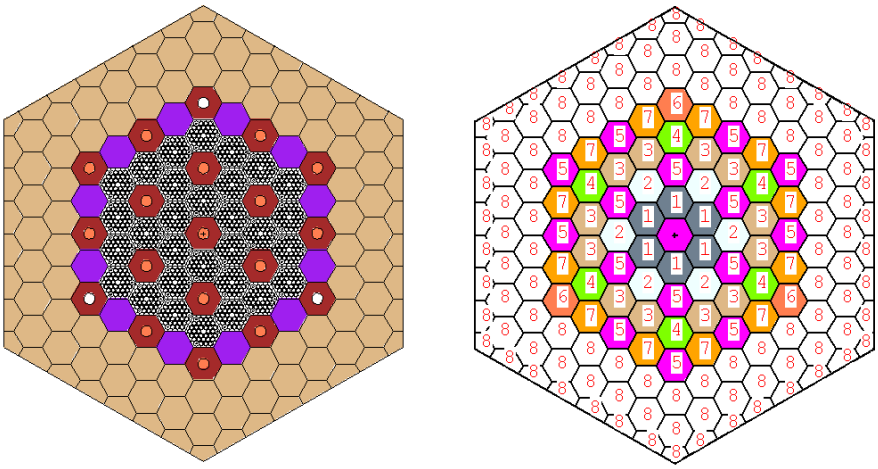

Figure 1. The whole core structure and configuration of the simplified HTTR benchmark. (a) Full core structure; (b) Region indexing in the full core.

The three fundamental block geometries are shown in Fig. 2: fuel blocks, reflector blocks, and control rod blocks. Each fuel block consists of 33 identical fuel pin cells and 3 burnable poison (BP) cells. The fuel enrichment within any single block is uniform but varies from block to block

within the core. Each control rod block contains a single removable control rod at its center. All geometric dimensions are listed in Table I.

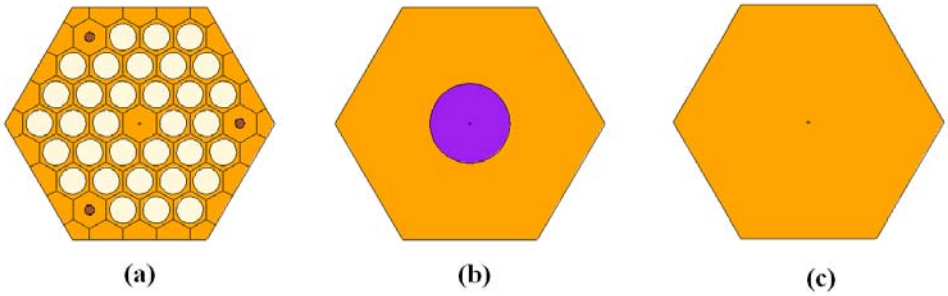

Figure 2. Block structures: (a) fuel blocks, (b) control rod blocks, (c) reflector blocks.

Table I. Simplified 2D HTTR benchmark geometry parameters

Number of fuel blocks	30
Number of replaceable reflector blocks	12
Number of permanent reflector blocks (whole/half/third blocks)	108 (66/36/6)
Flat-to-flat core width	436.4768 cm
Flat-to-flat block width	36 cm
Number of Fuel Pins per fuel block	33
Number of BP rods per fuel block	3
Flat-to-flat fuel pin cell width	5.15 cm
Fuel pin diameter	4.1 cm
BP rod diameter	1.5 cm
Control rod diameter	12.3 cm

2.3. Cross Section Data

A 6-group, transport corrected macroscopic cross section library was developed for the present benchmark problem consisting of four fuel cross sections (corresponding to the four enrichment levels found in the core), four graphite cross sections (corresponding to graphite in fuel blocks, in control rod blocks, and in permanent and replaceable reflector blocks), and cross sections for burnable poison pins and control rods. The number of cross section regions was intentionally

reduced to ten to promote the general usefulness of this benchmark for code development and verification. Increasing the number of cross section regions, while allowing for better agreement between this problem and the original benchmark, would increase the complexity of the problem description without contributing to underlying physics of the solution. The macroscopic cross section library was generated by a series of HELIOS [5] calculations. The energy group structure is shown in Table II. Each fuel pin was divided into several radial regions and six azimuthal regions in HELIOS for computational accuracy. Since HELIOS does not have helium in its cross section libraries vacuum is used instead of the helium coolant. This approximation is reasonable (acceptable) for the purpose of benchmarking neutronics methods. Intra-rod (pin) structures are explicitly described in the HELIOS calculations using the 190-group HELIOS cross section library. Three partial core structures for cross section calculations are described.

Table II. Energy Structure of Group Constants [6]

Group	Upper energy (eV)
1	1.00×10^{7}
2	1.83×10^{5}
3	9.61×10^{2}
4	2.38
5	0.65
6	0.105

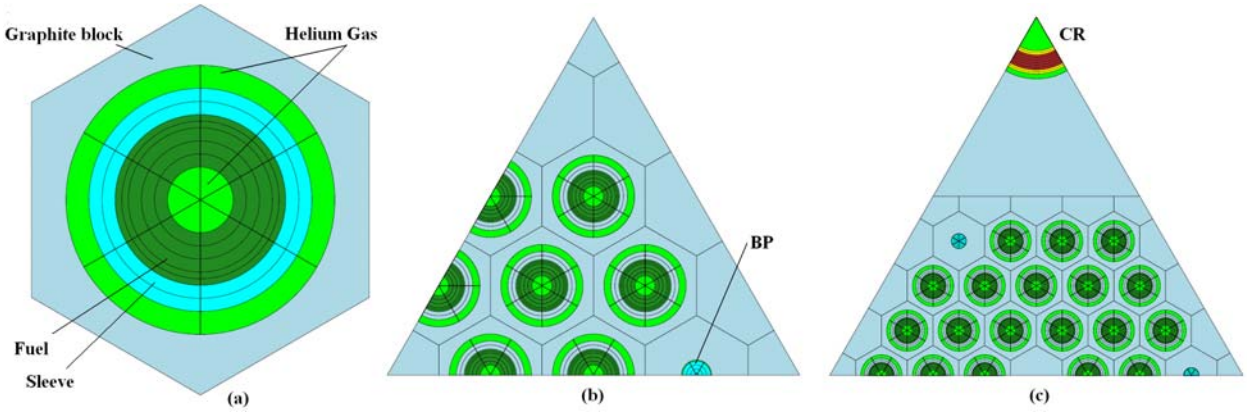

Figure 3. Partial core structures for cross section calculations.
(a) Fuel pin cell; (b) 1/6 fuel block; (c) 1/6 control rod block with half fuel block.

First, the four fuel cross sections were obtained by performing four pin cell calculations with specular reflection boundary conditions (shown in Figure 3(a)). For the sake of reducing the number of cross section regions in the present benchmark problem, however, the helium, fuel

and fuel sleeve regions were homogenized into a single macroscopic fuel material. The cross sections for graphite in fuel blocks are also generated in pin cell calculations.

Since the BP cells contain no fissionable material, it was necessary to use a larger section of the fuel block to obtain fluxes for collapsing the BP material. In this case, one-sixth of a fuel block was modeled (including a BP pin) with specular reflection boundary conditions (shown in Figure 3(b)).

Finally, macroscopic control rod cross sections were computed by modeling half of fuel block adjacent to a control rod block (shown in Figure 3(c)). The control rod cylinder was homogenized into a single control material and collapsed to the 6-group energy structure. Cross sections for reflector blocks are also calculated in similar geometry, replacing the 1/6 control rod block with 1/6 reflector block.

All HELIOS cross section calculations were performed with data of number densities and pin dimensions specified in Reference [1]. The fuel and BP materials are averaged axially, and BP and CR materials were diluted for the 2D benchmark problems to achieve reasonable core eigenvalues. Based on reference [7], typical operating temperatures for high temperature gas cooled reactors are used for different regions: 1130 K for fuel pins, 1080 K for fuel block and BP, and 853 K for other regions. The complete set of macroscopic cross sections is given in Appendix A, in which fuel type 1 to 4 correspond to fuel pin cross section data for region 1 to 4, respectively.

3. RESULTS

The benchmark solution was calculated by MCNP [8] with the 6-group cross section data described previously and given in tabular form in Appendix A. By symmetry, a 1/6 core model is sufficient for fully describing the problem solution. Three core configurations were considered corresponding to various control rod insertions as shown in Figure 4. Configuration 1 corresponds to the all-rods-in case. Configuration 2 is a partially controlled case with only some control rods inserted so that k_{eff} is close to one. Configuration 3 is an all-rods-out case. Figure 5 provides an indexing nomenclature at the block and pin level that will be used to describe the reference solution in subsequent discussions.

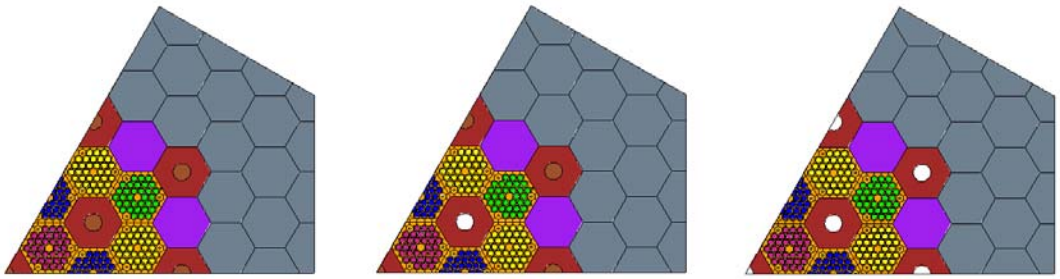

Figure 4. Reference benchmark problems.
(a) All-Rods-In Configuration; (b) Partially Controlled Configuration; (c) All-Rods-Out Configuration.

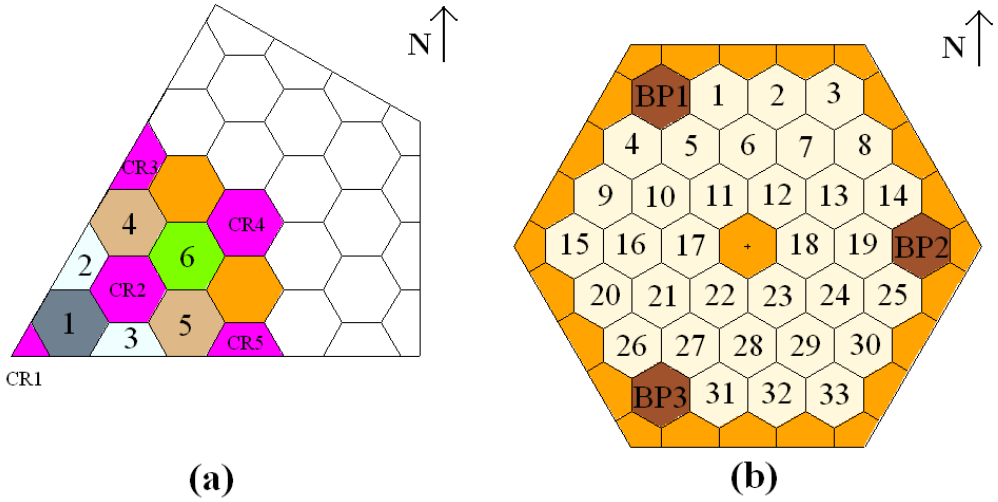

Figure 5. Block numbers and pin numbers for reference solutions.
(a) Block indexing in 1/6 core; (b) Pin indexing and BP indexing in one fuel block.

The MCNP reference solution for each configuration was obtained by first sampling 250 million neutron histories to generate the converged neutron fission source. An additional 500 million histories were sampled for tallying purposes. There are 30 fuel blocks containing a total of 990 fuel pins in the whole core. After symmetry reduction, there are 6 unique fuel blocks and 170 unique fuel pins in our reference problems. The eigenvalues (k_{eff}) of the three configurations are listed in Table III. The average and maximum pin fission density statistical uncertainties are shown in Table IV. Table V includes some specific pin fission densities data. Fuel block fission densities are provided in Table VI.

Table III. 6-group MCNP reference eigenvalue solutions

Benchmark configuration	Eigenvalue	Standard deviation
All Rods In	0.89623	0.00003
Partially Controlled	1.00391	0.00003
All Rods Out	1.09107	0.00003

Table IV. Pin fission density relative statistical uncertainty (%)

Benchmark configuration	AVG	MAX
All Rods In	0.02	0.03
Partially Controlled	0.02	0.03
All Rods Out	0.02	0.03

Table V. Relative statistical uncertainties for specific pin fission densities

Benchmark configuration	Maximum pin fission density	Uncertainty (%)	Minimum pin fission density	Uncertainty (%)
All Rods In	1.18089	0.02	0.85923	0.02
Partially Controlled	1.28795	0.02	0.79554	0.02
All Rods Out	1.20754	0.02	0.90014	0.02

Table VI. Fuel block averaged fission density distribution

Block Number	Fuel Type Number	Case 1	Case 2	Case 3
1	1	1.02250	1.00557	0.96113
2*	2	1.05680	1.11166	1.01115
3*	2	1.05784	1.11213	1.01180
4	3	0.97819	0.96839	1.00187
5	3	0.98053	0.97015	1.00321
6	4	0.96146	0.94399	1.02230

* Half blocks on the reflective boundaries

The complete set of pin fission densities and their standard deviations are presented in Appendix B. These fission densities were normalized to the total number of fuel pins in the whole core (i.e. the total sum of fission densities is 990.) Absorption rates in every burnable poison pin and control rod are also presented in Appendix B normalized by the whole core fission rate as $A_i = \Sigma_{a,i}\varphi_i V_i \Big/ \sum_{j=1}^{990} \Sigma_{f,j}\varphi_j V_j$, in which, *i* and *j* are indices for absorber rod and fuel pins respectively, and Σ, ϕ, and *V* represent the corresponding cross section, flux and volume.

4. CONCLUSIONS

A 2D HTTR benchmark (in three configurations) has been presented to support the development of new full-core methods for hexagonal NGNP reactor designs. Simplifications were made from the original HTTR start-up benchmark to simplify the problem description while preserving the fundamental physics of the reactor. A complete six-group cross section library has been provided in addition to precise Monte Carlo reference solutions for each configuration. This benchmark problem will serve as valuable test cases for the development of new computational methods for emerging high temperature reactor core designs.

ACKNOWLEDGMENTS

The authors would like to thank Dr. T.A. Taiwo, Dr. T.K. Kim, and Dr. A. Baxter for their help on the authors' literature search for the benchmark problem. Funding for this work was provided by a Department of Energy Nuclear Energy Research Initiative Grant # DE-FC07-07ID14821.

REFERENCES

1. N. Nojiri, N. Nakano, et al, "Benchmark Problem's Data for HTTR's Start-up Core Physics Experiments" *JAERI-memo 10-1005*, Japan (1998).
2. T. A. Taiwo, T. K. Kim, et al, "Evaluation of High Temperature Gas-Cooled Reactor", *ANL-GenIV-059* (2005)
3. "Evaluation of High Temperature Gas Cooled Reactor Performance: Benchmark analysis related to initial testing of the HTTR and HTR-10," *IAEA-TECDOC-1382*, IAEA (2003).
4. X. Raepsaet et al. "Analysis of the European Results on the HTTR's Core Physics Benchmarks," *Nuclear Engineering and Design*, **222**, pp.173-187 (2003).
5. T. Simeonov, "Release Notes - Helios System Version 1.8," Studsvik Scandpower Report, *SSP-03/221*, November 26 (2003).
6. I. Murata, K. Yamashita, et al, "Evaluation of Local Power Distribution with Fine-mesh Core Model for High Temperature Engineering Test Reactor (HTTR)", *Journal of Nuclear Science and Technology*, **31(1)**, pp.62-72, (1994)
7. A. Baxter (General Atomics), Email Communication with F. Rahnema, December 16, (2008)
8. X-5 Monte Carlo Team "MCNP - A General Monte Carlo N-Particle Transport Code, Version 5" Los Alamos National Laboratory, *LA-CP-03-0245* (2003).

APPENDIX A. A 6-group cross section library for simplified HTTR benchmark

Table VII(a). Fuel type 1 macroscopic cross sections

Group	total	transport	absorption	capture	fission	chi	nu
1	1.57584E-01	1.40279E-01	2.15574E-04	6.96870E-05	1.45887E-04	9.69182E-01	2.72065E+00
2	2.53859E-01	2.39022E-01	5.95068E-04	4.93997E-04	1.01071E-04	3.08180E-02	2.43248E+00
3	2.68697E-01	2.54817E-01	7.56124E-03	6.69570E-03	8.65544E-04	0.00000E+00	2.43380E+00
4	2.58719E-01	2.44406E-01	1.94937E-03	6.82030E-04	1.26734E-03	0.00000E+00	2.43379E+00
5	2.66603E-01	2.52191E-01	6.63838E-03	1.61371E-03	5.02467E-03	0.00000E+00	2.43379E+00
6	2.89881E-01	2.76274E-01	1.43368E-02	3.21190E-03	1.11249E-02	0.00000E+00	2.43380E+00

Scattering matrix:

FUEL1	to Group 1	to Group 2	to Group 3	to Group 4	to Group 5	to Group 6
Group 1	1.29880E-01	1.40279E-01	6.40149E-09	0.00000E+00	0.00000E+00	0.00000E+00
Group 2	0.00000E+00	2.31378E-01	7.04916E-03	0.00000E+00	0.00000E+00	0.00000E+00
Group 3	0.00000E+00	0.00000E+00	2.42620E-01	4.63580E-03	0.00000E+00	0.00000E+00
Group 4	0.00000E+00	0.00000E+00	1.15590E-04	2.06563E-01	3.57760E-02	2.13346E-06
Group 5	0.00000E+00	0.00000E+00	0.00000E+00	3.05160E-03	2.16501E-01	2.60003E-02
Group 6	0.00000E+00	0.00000E+00	0.00000E+00	5.25354E-07	6.63488E-02	1.95588E-01

Table VII(b). Fuel type 2 macroscopic cross sections

Group	total	transport	absorption	capture	fission	chi	nu
1	1.57399E-01	1.40123E-01	2.20776E-04	6.96870E-05	1.51089E-04	9.69204E-01	2.71368E+00
2	2.53589E-01	2.38764E-01	6.13298E-04	4.95267E-04	1.18031E-04	3.07961E-02	2.43246E+00
3	2.68591E-01	2.54725E-01	7.74058E-03	6.73258E-03	1.00800E-03	0.00000E+00	2.43381E+00
4	2.58716E-01	2.44417E-01	2.20770E-03	7.31840E-04	1.47586E-03	0.00000E+00	2.43379E+00
5	2.67149E-01	2.52754E-01	7.56962E-03	1.74828E-03	5.82134E-03	0.00000E+00	2.43380E+00
6	2.91369E-01	2.77777E-01	1.64203E-02	3.48970E-03	1.29306E-02	0.00000E+00	2.43380E+00

Scattering matrix:

FUEL2	to Group 1	to Group 2	to Group 3	to Group 4	to Group 5	to Group 6
Group 1	1.29739E-01	1.01637E-02	6.32931E-09	0.00000E+00	0.00000E+00	0.00000E+00
Group 2	0.00000E+00	2.31131E-01	7.02000E-03	0.00000E+00	0.00000E+00	0.00000E+00
Group 3	0.00000E+00	0.00000E+00	2.42407E-01	4.57763E-03	0.00000E+00	0.00000E+00
Group 4	0.00000E+00	0.00000E+00	1.16470E-04	2.06858E-01	3.52328E-02	2.08456E-06
Group 5	0.00000E+00	0.00000E+00	0.00000E+00	3.25353E-03	2.16576E-01	2.53550E-02
Group 6	0.00000E+00	0.00000E+00	0.00000E+00	5.27219E-07	6.64234E-02	1.94933E-01

Table VII(c). Fuel type 3 macroscopic cross sections

Group	total	transport	absorption	capture	fission	chi	nu
1	1.57341E-01	1.40079E-01	2.25694E-04	6.95260E-05	1.56168E-04	9.69222E-01	2.70660E+00
2	2.53475E-01	2.38652E-01	6.30989E-04	4.94727E-04	1.36262E-04	3.07778E-02	2.43246E+00
3	2.68658E-01	2.54794E-01	7.92286E-03	6.76242E-03	1.16044E-03	0.00000E+00	2.43379E+00
4	2.58900E-01	2.44605E-01	2.48390E-03	7.84470E-04	1.69943E-03	0.00000E+00	2.43379E+00
5	2.67922E-01	2.53531E-01	8.55481E-03	1.88906E-03	6.66575E-03	0.00000E+00	2.43380E+00
6	2.93159E-01	2.79573E-01	1.86348E-02	3.78210E-03	1.48527E-02	0.00000E+00	2.43379E+00

Scattering matrix:

FUEL3	to Group 1	to Group 2	to Group 3	to Group 4	to Group 5	to Group 6
Group 1	1.29700E-01	1.01528E-02	6.35128E-09	0.00000E+00	0.00000E+00	0.00000E+00
Group 2	0.00000E+00	2.31024E-01	6.99712E-03	0.00000E+00	0.00000E+00	0.00000E+00
Group 3	0.00000E+00	0.00000E+00	2.42347E-01	4.52380E-03	0.00000E+00	0.00000E+00
Group 4	0.00000E+00	0.00000E+00	1.17088E-04	2.07221E-01	3.47808E-02	2.04390E-06
Group 5	0.00000E+00	0.00000E+00	0.00000E+00	3.45980E-03	2.16787E-01	2.47297E-02
Group 6	0.00000E+00	0.00000E+00	0.00000E+00	5.29569E-07	6.65506E-02	1.94387E-01

Table VII(d). Fuel type 4 macroscopic cross sections

Group	total	transport	absorption	capture	fission	chi	nu
1	1.57526E-01	1.40246E-01	2.30645E-04	6.99520E-05	1.60693E-04	9.69230E-01	2.70289E+00
2	2.53890E-01	2.39043E-01	6.47492E-04	4.99466E-04	1.48026E-04	3.07695E-02	2.43245E+00
3	2.69220E-01	2.55337E-01	8.07560E-03	6.81751E-03	1.25809E-03	0.00000E+00	2.43380E+00
4	2.59479E-01	2.45164E-01	2.66509E-03	8.21720E-04	1.84337E-03	0.00000E+00	2.43380E+00
5	2.68870E-01	2.54459E-01	9.18852E-03	1.98437E-03	7.20415E-03	0.00000E+00	2.43381E+00
6	2.94804E-01	2.81201E-01	2.00629E-02	3.98050E-03	1.60824E-02	0.00000E+00	2.43379E+00

Scattering matrix:

FUEL4	to Group 1	to Group 2	to Group 3	to Group 4	to Group 5	to Group 6
Group 1	1.29854E-01	1.01609E-02	6.24522E-09	0.00000E+00	0.00000E+00	0.00000E+00
Group 2	0.00000E+00	2.31400E-01	6.99578E-03	0.00000E+00	0.00000E+00	0.00000E+00
Group 3	0.00000E+00	0.00000E+00	2.42768E-01	4.49327E-03	0.00000E+00	0.00000E+00
Group 4	0.00000E+00	0.00000E+00	1.18056E-04	2.07787E-01	3.45918E-02	2.02519E-06
Group 5	0.00000E+00	0.00000E+00	0.00000E+00	3.59085E-03	2.17288E-01	2.43920E-02
Group 6	0.00000E+00	0.00000E+00	0.00000E+00	5.31868E-07	6.67394E-02	1.94398E-01

Table VII(e). Macroscopic cross sections of graphite in fuel blocks and control rod blocks

Graphite in Fuel Blocks (GFB)				Graphite in Control Rod Block (GCRB)			
Group	**total**	**transport**	**absorption**	**Group**	**total**	**transport**	**absorption**
1	2.49600E-01	2.24250E-01	4.67717E-07	**1**	2.56162E-01	2.29929E-01	4.60312E-07
2	4.09764E-01	3.84979E-01	5.55447E-07	**2**	4.10803E-01	3.86138E-01	6.00313E-07
3	4.20603E-01	3.97025E-01	9.33010E-06	**3**	4.20612E-01	3.97035E-01	1.06080E-05
4	4.22094E-01	3.97845E-01	4.86553E-05	**4**	4.21754E-01	3.97573E-01	4.83129E-05
5	4.28111E-01	4.03633E-01	1.08625E-04	**5**	4.27015E-01	4.02580E-01	1.13842E-04
6	4.56053E-01	4.32806E-01	2.26992E-04	**6**	4.50217E-01	4.26725E-01	2.33122E-04

Scattering matrix:

GFB	to Group 1	to Group 2	to Group 3	to Group 4	to Group 5	to Group 6
Group 1	2.07175E-01	1.70746E-02	0.00000E+00	0.00000E+00	0.00000E+00	0.00000E+00
Group 2	0.00000E+00	3.73010E-01	1.19682E-02	0.00000E+00	0.00000E+00	0.00000E+00
Group 3	0.00000E+00	0.00000E+00	3.89230E-01	7.78561E-03	0.00000E+00	0.00000E+00
Group 4	0.00000E+00	0.00000E+00	9.42066E-05	3.37330E-01	6.03694E-02	2.65156E-06
Group 5	0.00000E+00	0.00000E+00	0.00000E+00	4.82402E-03	3.54747E-01	4.39538E-02
Group 6	0.00000E+00	0.00000E+00	0.00000E+00	2.50273E-07	1.08894E-01	3.23685E-01

GCRB	to Group 1	to Group 2	to Group 3	to Group 4	to Group 5	to Group 6
Group 1	2.09984E-01	1.99447E-02	0.00000E+00	0.00000E+00	0.00000E+00	0.00000E+00
Group 2	0.00000E+00	3.72537E-01	1.36000E-02	0.00000E+00	0.00000E+00	0.00000E+00
Group 3	0.00000E+00	0.00000E+00	3.86688E-01	1.03363E-02	0.00000E+00	0.00000E+00
Group 4	0.00000E+00	0.00000E+00	4.03889E-05	3.40580E-01	5.69036E-02	8.34122E-07
Group 5	0.00000E+00	0.00000E+00	0.00000E+00	2.30775E-03	3.46856E-01	5.33025E-02
Group 6	0.00000E+00	0.00000E+00	0.00000E+00	0.00000E+00	8.33229E-02	3.43169E-01

Table VII(f). Macroscopic cross sections of reflectors

Replaceable Reflector (graphite) (RPRFL)				Permanent Reflector (graphite) (PMRFL)			
Group	**total**	**transport**	**absorption**	**Group**	**total**	**transport**	**absorption**
1	2.56681E-01	2.30464E-01	4.45761E-07	**1**	2.49338E-01	2.23870E-01	4.51811E-07
2	4.10741E-01	3.86068E-01	5.97054E-07	**2**	3.99100E-01	3.75125E-01	7.81616E-07
3	4.20612E-01	3.97035E-01	1.06098E-05	**3**	4.08705E-01	3.85796E-01	1.38175E-05
4	4.21757E-01	3.97575E-01	4.83861E-05	**4**	4.09831E-01	3.86333E-01	6.31098E-05
5	4.27167E-01	4.02738E-01	1.15337E-04	**5**	4.15102E-01	3.91363E-01	1.50359E-04
6	4.50510E-01	4.27039E-01	2.34136E-04	**6**	4.37814E-01	4.15006E-01	3.05738E-04

Scattering matrix:

RPRFL	to Group 1	to Group 2	to Group 3	to Group 4	to Group 5	to Group 6
Group 1	2.10472E-01	1.99918E-02	0.00000E+00	0.00000E+00	0.00000E+00	0.00000E+00
Group 2	0.00000E+00	3.72599E-01	1.34684E-02	0.00000E+00	0.00000E+00	0.00000E+00
Group 3	0.00000E+00	0.00000E+00	3.86633E-01	1.03913E-02	0.00000E+00	0.00000E+00
Group 4	0.00000E+00	0.00000E+00	4.00763E-05	3.39817E-01	5.76690E-02	8.53907E-07
Group 5	0.00000E+00	0.00000E+00	0.00000E+00	1.91158E-03	3.44655E-01	5.60563E-02
Group 6	0.00000E+00	0.00000E+00	0.00000E+00	0.00000E+00	8.26248E-02	3.44180E-01

PMRFL	to Group 1	to Group 2	to Group 3	to Group 4	to Group 5	to Group 6
Group 1	2.04473E-01	1.93969E-02	0.00000E+00	0.00000E+00	0.00000E+00	0.00000E+00
Group 2	0.00000E+00	3.62056E-01	1.30685E-02	0.00000E+00	0.00000E+00	0.00000E+00
Group 3	0.00000E+00	0.00000E+00	3.75706E-01	1.00761E-02	0.00000E+00	0.00000E+00
Group 4	0.00000E+00	0.00000E+00	3.89546E-05	3.30218E-01	5.60120E-02	8.29063E-07
Group 5	0.00000E+00	0.00000E+00	0.00000E+00	1.87786E-03	3.35030E-01	5.43044E-02
Group 6	0.00000E+00	0.00000E+00	0.00000E+00	0.00000E+00	8.03266E-02	3.34374E-01

Table VII(g). Macroscopic cross sections of absorber in BP and CR

Burnable poison Rod (BP)				Control Rod (CR)			
Group	**total**	**transport**	**absorption**	**Group**	**total**	**transport**	**absorption**
1	1.11202E-01	9.98495E-02	9.12361E-05	**1**	1.62226E-03	1.41377E-03	1.81632E-05
2	1.81675E-01	1.70767E-01	9.94124E-04	**2**	3.69733E-03	3.56840E-03	1.73749E-04
3	2.02033E-01	1.91637E-01	1.68800E-02	**3**	6.37189E-03	6.25553E-03	2.85937E-03
4	2.67859E-01	2.57202E-01	8.26921E-02	**4**	1.64585E-02	1.63384E-02	1.29936E-02
5	3.71702E-01	3.61004E-01	1.84961E-01	**5**	3.32218E-02	3.31026E-02	2.97540E-02
6	5.65046E-01	5.54913E-01	3.69756E-01	**6**	6.01351E-02	6.00227E-02	5.65912E-02

Scattering matrix:

BP	to Group 1	to Group 2	to Group 3	to Group 4	to Group 5	to Group 6
Group 1	9.18089E-02	7.94934E-03	0.00000E+00	0.00000E+00	0.00000E+00	0.00000E+00
Group 2	0.00000E+00	1.64351E-01	5.42194E-03	0.00000E+00	0.00000E+00	0.00000E+00
Group 3	0.00000E+00	0.00000E+00	1.70885E-01	3.87196E-03	0.00000E+00	0.00000E+00
Group 4	0.00000E+00	0.00000E+00	4.83109E-05	1.47886E-01	2.65742E-02	1.01983E-06
Group 5	0.00000E+00	0.00000E+00	0.00000E+00	1.86197E-03	1.54683E-01	1.94979E-02
Group 6	0.00000E+00	0.00000E+00	0.00000E+00	0.00000E+00	4.81034E-02	1.37054E-01

CR	to Group 1	to Group 2	to Group 3	to Group 4	to Group 5	to Group 6
Group 1	1.29669E-03	9.89118E-05	4.53299E-12	0.00000E+00	0.00000E+00	0.00000E+00
Group 2	0.00000E+00	3.32805E-03	6.65993E-05	0.00000E+00	0.00000E+00	0.00000E+00
Group 3	0.00000E+00	0.00000E+00	3.34736E-03	4.88000E-05	0.00000E+00	0.00000E+00
Group 4	0.00000E+00	0.00000E+00	5.35782E-06	3.04316E-03	2.96282E-04	3.94986E-09
Group 5	0.00000E+00	0.00000E+00	0.00000E+00	1.73324E-05	3.03479E-03	2.96474E-04
Group 6	0.00000E+00	0.00000E+00	0.00000E+00	0.00000E+00	5.12212E-04	2.91929E-03

Appendix B. Reference pin fission densities for three benchmark configurations

Table VIII. Fuel pin number map (see Fig. 5b)

			BP1	1	2	3
		4	5	6	7	8
	9	10	11	12	13	14
15	16	17	Center	18	19	BP2
20	21	22	23	24	2S5	
26	27	28	29	30		
BP3	31	32	33			

Table IX(a). Fuel pin fission density distribution in Block 1, Configuration 1.

			BP1	0.99037	1.01622	1.06129
		1.01191	0.98254	0.98929	1.00825	1.05518
	1.05615	1.00773	0.99503	0.99453	1.00180	1.03755
1.11969	1.04399	1.01172	Center	0.99219	0.98932	BP2
1.10872	1.03564	1.00902	0.99748	0.99035	0.99808	
1.08925	1.02195	1.00752	1.00414	1.01258		
BP3	1.03379	1.03255	1.03665			

Table IX(b). Fuel pin fission density distribution in Block 2, Configuration 1.

			BP1			0.98532
					0.97855	0.98599
				0.99797	0.98803	0.99825
			Center	1.01586	1.01449	BP2
		1.04761	1.04394	1.05230	1.09788	
	1.06189	1.06570	1.08664	1.14221		
BP3	1.10104	1.12826	**1.18089**			

Table IX(c). Fuel pin fission density distribution in Block 3, Configuration 1.

			BP1	1.12206	1.11245	1.09349
		1.10869	1.06541	1.05146	1.03405	1.01980
	1.12544	1.06765	1.04242	1.01930	0.99109	0.97248
1.15707	1.08596	1.05134	Center	0.99806	0.96477	BP2
BP3						

Table IX(d). Fuel pin fission density distribution in Block 4, Configuration 1.

			BP1	0.93514	0.95590	1.01132
		0.94273	0.90792	0.90909	0.93068	0.99874
	0.98519	0.93211	0.91652	0.91447	0.92802	0.98966
1.04542	0.97668	0.94627	Center	0.92451	0.92805	BP2
1.04557	0.98789	0.96656	0.95327	0.94126	0.95219	
1.06149	1.01693	1.00442	0.99324	0.99279		
BP3	1.10779	1.09665	1.08176			

Table IX(e). Fuel pin fission density distribution in Block 5, Configuration 1.

			BP1	0.97667	0.96982	1.01568
		1.08744	0.97907	0.94355	0.94640	1.00679
	1.12856	1.00916	0.95381	0.92901	0.93078	0.98907
1.16861	1.04076	0.97233	Center	0.91435	0.91691	BP2
1.08443	0.99106	0.94520	0.91870	0.90990	0.94277	
1.03207	0.95986	0.93096	0.92230	0.94914		
BP3	0.96585	0.95533	0.97116			

Table IX(f). Fuel pin fission density distribution in Block 6, Configuration 1.

			BP1	0.99363	0.97362	0.95912
		0.98735	0.93084	0.90526	0.88601	0.89242
	1.03013	0.94626	0.90495	0.87656	0.85923	0.88063
1.12659	1.00154	0.93640	Center	0.87565	0.87434	BP2
1.11140	0.98991	0.93482	0.90877	0.90897	0.96746	
1.09721	0.98463	0.94734	0.95050	1.01342		
BP3	1.01334	1.00510	1.05491			

Table X(a). Fuel pin fission density distribution in Block 1, Configuration 2.

			BP1	0.98590	1.04553	1.14505
		0.96686	0.95632	0.98863	1.04616	1.15037
	0.99362	0.96126	0.96850	0.99600	1.04102	1.13086
1.03980	0.97975	0.96377	Center	0.99241	1.02140	BP2
1.02754	0.97100	0.96122	0.97002	0.98602	1.01909	
1.00934	0.95931	0.96064	0.97518	1.00343		
BP3	0.97305	0.98719	1.00755			

Table X(b). Fuel pin fission density distribution in Block 2, Configuration 2.

			BP1			0.99127
					0.99948	1.00526
				1.03029	1.02210	1.04444
			Center	1.05946	1.07854	BP2
		1.07970	1.08805	1.12522	1.22295	
	1.08159	1.10020	1.15356	1.26796		
BP3	1.11795	1.17753	**1.28795**			

Table X(c). Fuel pin fission density distribution in Block 3, Configuration 2.

			BP1	1.24566	1.23885	1.20343
		1.14869	1.12655	1.12375	1.10275	1.07449
	1.13639	1.09713	1.08403	1.06411	1.02934	0.99716
1.15212	1.10054	1.08005	Center	1.03298	0.98998	BP2
BP3						

Table X(d). Fuel pin fission density distribution in Block 4, Configuration 2.

			BP1	0.86491	0.88004	0.92687
		0.89114	0.85384	0.85064	0.86608	0.92393
	0.94854	0.89405	0.87532	0.86922	0.87680	0.92629
1.02652	0.95720	0.92741	Center	0.89928	0.89375	BP2
1.04822	0.99527	0.97805	0.96239	0.94203	0.93832	
1.09956	1.06747	1.06124	1.04277	1.02487		
BP3	1.23457	1.22259	1.18766			

Table X(e). Fuel pin fission density distribution in Block 5, Configuration 2.

			BP1	0.99960	0.94908	0.96214
		1.21158	1.02271	0.93894	0.90803	0.94154
	1.25738	1.06538	0.96100	0.90113	0.87841	0.91474
1.28351	1.09649	0.98471	Center	0.86869	0.85367	BP2
1.13192	1.00273	0.92805	0.87824	0.85157	0.86827	
1.03992	0.94259	0.89297	0.86725	0.87839		
BP3	0.92900	0.90251	0.90300			

Table X(f). Fuel pin fission density distribution in Block 6, Configuration 2.

			BP1	0.92794	0.89729	0.87465
		0.97211	0.89482	0.85163	0.81966	0.81508
	1.06392	0.94553	0.87692	0.82705	0.79554	0.80366
1.23751	1.05179	0.94272	Center	0.82642	0.80869	BP2
1.24263	1.04482	0.93885	0.87864	0.85440	0.89107	
1.22691	1.02808	0.94123	0.91006	0.94519		
BP3	1.03669	0.98289	0.99736			

Table XI(a). Fuel pin fission density distribution in Block 1, Configuration 3.

			BP1	0.90935	0.95530	1.03982
		0.92836	0.90014	0.91578	0.95748	1.04599
	0.99153	0.93261	0.91652	0.92445	0.95399	1.02850
1.09431	0.99067	0.94028	Center	0.92102	0.93534	BP2
1.09754	0.98515	0.93612	0.91676	0.91296	0.93126	
1.07776	0.96543	0.92801	0.91582	0.92498		
BP3	0.96310	0.94230	0.93875			

Table XI(b). Fuel pin fission density distribution in Block 2, Configuration 3.

			BP1			0.92532
					0.91990	0.93124
				0.93848	0.93554	0.96126
			Center	0.96178	0.98237	BP2
		0.97482	0.98390	1.01905	1.11104	
	0.97855	0.99454	1.04260	1.14769		
BP3	1.01437	1.06566	1.16442			

Table XI(c). Fuel pin fission density distribution in Block 3, Configuration 3.

			BP1	1.12746	1.12694	1.10205
		1.03980	1.01824	1.01842	1.00468	0.98834
	1.03147	0.99145	0.98005	0.96607	0.94134	0.92247
1.04984	0.99633	0.97604	Center	0.94028	0.90952	BP2
BP3						

Table XI(d). Fuel pin fission density distribution in Block 4, Configuration 3.

			BP1	1.03328	1.07199	1.13681
		0.94870	0.93747	0.95936	0.99368	1.07134
	0.95686	0.92315	0.92525	0.93749	0.96148	1.03169
0.99692	0.94546	0.93211	Center	0.93651	0.94655	BP2
1.00324	0.96525	0.96113	0.96024	0.95507	0.96770	
1.03958	1.01949	1.02513	1.02079	1.01920		
BP3	1.16561	1.16626	1.14693			

Table XI(e). Fuel pin fission density distribution in Block 5, Configuration 3.

			BP1	0.99752	0.98265	1.03821
		1.15465	1.00223	0.95307	0.96189	1.04372
	1.18621	1.02880	0.95887	0.93772	0.95915	1.05234
1.20022	1.04658	0.96759	Center	0.93471	0.97247	BP2
1.06888	0.97226	0.93351	0.92838	0.95805	1.05423	
0.99436	0.93306	0.92594	0.95611	1.04689		
BP3	0.94330	0.96850	1.04401			

Table XI(f). Fuel pin fission density distribution in Block 6, Configuration 3.

			BP1	1.04992	1.06471	1.10654
		1.01229	0.96435	0.95924	0.97502	1.03976
	1.06817	0.97691	0.94028	0.92964	0.94648	1.02428
1.20699	1.05004	0.97003	Center	0.92760	0.95685	BP2
1.20754	1.04138	0.96701	0.94183	0.95874	1.05024	
1.19272	1.02869	0.97470	0.98096	1.06449		
BP3	1.04546	1.02732	1.08591			

* All relative standard deviations are 0.0002 to 0.0003.

** In block 2 and 3, half fuel pin fission densities on the boundary are doubled by symmetry, blanks in the table can be completed according to symmetry.

** In block 2 and 3, half fuel pin fission densities on the boundary are doubled by symmetry, blanks in the table can be completed according to symmetry.

Table XII. Burnable poison absorption rate in three configurations

		FB 1	FB 2	FB 3	FB 4	FB 5	FB 6
Case 1	BP1	5.81165E-04	5.36668E-04*	5.78834E-04	4.18763E-04	4.68745E-04	4.20741E-04
	BP2	5.99689E-04	5.36668E-04	4.83525E-04**	4.36828E-04	4.38074E-04	3.86003E-04
	BP3	6.30980E-04	5.61912E-04**	5.78834E-04*	5.02140E-04	4.49502E-04	4.51855E-04
Case 2	BP1	5.66541E-04	5.89842E-04*	6.29725E-04	3.89680E-04	5.12877E-04	3.99482E-04
	BP2	6.45211E-04	5.89842E-04	4.88490E-04**	4.15350E-04	4.01663E-04	3.52147E-04
	BP3	5.86466E-04	5.62556E-04**	6.29725E-04*	5.50737E-04	4.42108E-04	4.95324E-04
Case 3	BP1	5.29122E-04	5.39946E-04*	5.69587E-04	4.49941E-04	4.95898E-04	4.35194E-04
	BP2	5.86399E-04	5.39946E-04	4.56255E-04**	4.48890E-04	4.90500E-04	4.44164E-04
	BP3	6.15850E-04	5.13074E-04**	5.69587E-04*	5.15467E-04	4.30446E-04	4.83939E-04

* Missed in 1/6 core geometry, completed by symmetry.
** Half BP rod in 1/6 core geometry, doubled by symmetry.

Table XIII. Control rods absorption rate in three configurations

	CR 1	CR 2	CR 3	CR 4	CR 5
Case 1	3.95432E-02	3.39651E-02	2.14362E-02	1.58424E-02	2.13977E-02
Case 2	3.58724E-02	-	1.92058E-02	1.40895E-02	1.91687E-02
Case 3	-	-	-	-	-